Tailoring Optical Fields Emitted by Subwavelength Nanometric Sources

**Raúl A. Bustos-Marún · Axel D. Dente ·
Eduardo A. Coronado · Horacio M. Pastawski**

Abstract In this work, we study a simple way of controlling the emitted fields of subwavelength nanometric sources. The system studied consists of arrays of nanoparticles (NPs) embedded in optical active media. The key concept is the careful tuning of NP's damping factors, which changes the eigenmode's decay rates of the whole array. This inevitably leads, at long time, to a locking of relative phases and frequencies of individual localized-surfaces-plasmons (LSPs) and, thus, controls the emitted field. The amplitude of the LSP's oscillations can be kept constant by embedding the system in optical active media. In the case of full loss compensation, this implies that not only the relative phases, but also the amplitudes of the LSPs remain fixed, leading us, additionally, to interpret the process as a new example of synchronization. The proposed approach can be used as a general way of controlling and designing the electromagnetic fields emitted by nanometric sources, which can find applications in optoelectronic, nanoscale lithography, and probing microscopy.

Keywords Plasmonics · Localized-surface-plasmons · Nanoparticles · Active medium · Synchronization

R. A. Bustos-Marún (✉) · A. D. Dente · H. M. Pastawski
Instituto de Física Enrique Gaviola (IFEG), CONICET-UNC
and Facultad de Matemática, Astronomía y Física, Universidad
Nacional de Córdoba, 5000 Córdoba, Argentina
e-mail: rbustos@famaf.unc.edu.ar

A. D. Dente
e-mail: dente@famaf.unc.edu.ar

H. M. Pastawski
e-mail: horacio@famaf.unc.edu.ar

E. A. Coronado
INFIQC, Departamento de Fisicoquímica, Facultad de Ciencias
Químicas, UNC, Ciudad Universitaria, Córdoba, Argentina
e-mail: coronado@fcq.unc.edu.ar

R. A. Bustos-Marún
Departamento de Fisicoquímica, Facultad Ciencias Químicas,
UNC, Ciudad Universitaria, 5000 Córdoba, Argentina

A. D. Dente
INVAP S.E., 8403, San Carlos de Bariloche, Argentina

Introduction

Recent advances in the past decades in fabrication and characterization of nanometric devices have given rise to a revolution, fueled by the new and intriguing properties of matter in this size scale. Among the new fields that rapidly became central, emerged the promise of plasmonics with applications that go from ultrasensitive nanosensors to plasmonic circuitry [1–5]. Many of those promises have became a reality nowadays, but the advances do not seem to slow down and new ideas are still emerging in this field. One interesting example is the combination of plasmonic devices with active media that compensate in part or totally system's losses [6–25].

Active media are made of dye molecules or semiconductors nanocrystals, where the population inversion is created optically or electrically. The concept of surface plasmon amplification by stimulated emission of radiation (spaser), also known as surface plasmon laser in a wider context, is an example of that. Originally proposed by Bergman and Stockman in 2003 [14], and finally implemented experimentally in 2009 [18–20], it is basically a source of

electromagnetic fields, containing both propagating and evanescent waves, and formed by the interaction of surface plasmons with active media that fully compensate the losses of the plasmonics system [14–17].

Spasers can provide us with many possibilities for prospective applications in nanoscience and nanotechnology, in particular for near-field nonlinear-optical probing and nanomodification. In this respect, it should be desirable to control and to design a priori the electromagnetic fields generated by those hybrid systems. If the plasmonic system consist of arrays of NPs, the design of electromagnetic fields implies a control over the synchronized oscillation of the individual localized surface plasmons (LSPs), which leads to another interesting aspect. Essentially, as in those systems, not only the phases and frequencies of individual LSPs but also their amplitudes remain fixed; the whole phenomenon can be interpreted as another example of synchronization.

The phenomenon of synchronization, usually defined as the adjustment of rhythms of self-sustained oscillating objects because of their mutual interaction [26], has been observed in many physical and biological systems: from the coupled pendulums clocks first described by Christian Huygens [27] to the chemical or biological examples, such as fireflies that flash in unison [26]. However, to our knowledge, it has never been described in the context of plasmonics.

In this work, we study plasmonic systems, consisting of metallic nanoparticle (NP) arrays, where losses are partially or fully compensated by an active medium. We not only find that the localized surface plasmons (LSPs) of individual NPs can be kept oscillating with a fixed amplitude and a fixed relative phase, becoming a new example of synchronization, but we also show that it should be relatively easy to control their asymptotic states by controlling NP's damping. The manipulation of the system's state at long time implies the control of NP's dipolar moments and thus of their emitted electromagnetic field. Therefore, our approach is a general way of designing the interference patterns of sources of optical fields in the subwavelength scale, which can have applications in several areas of nanotechnology.

The paper is organized as follows: In "Coupled Dipole Approximation for Ellipsoids with Radiation Damping," we develop the basics tools used in our calculation. In "Results," we present the main results, analyzed through two simple examples of NP's arrays, and discuss them in terms of non-Hermiticity of the dynamical matrix and asymptotic states, phase and frequency locking, role of active media, gain-loss compensation, amplitude locking, and generalization to more complex structures. Finally, in "Conclusions," we summarize the main conclusions.

Coupled Dipole Approximation for Ellipsoids with Radiation Damping

The systems studied are basically different arrays of metallic NPs which are modeled through the well-known coupled dipole approximation [28–34]. In this model, each ith-NP is described by a dipole $\mathbf{P}_i$ induced by the electric field produced by the other dipoles, $\mathbf{E}_{j,i}$, and the external source, $\mathbf{E}_i^{(\text{ext})}$. We assume a generic ellipsoidal shape for the NPs whose polarizabilities α are described in a quasi-static approximation [35, 36],

$$\alpha = \frac{\epsilon_0 V (\epsilon - \epsilon_m)}{[\epsilon_m + L(\epsilon - \epsilon_m)]}, \tag{1}$$

where V is the volume, ϵ_0 is the free space permittivity, ϵ_m is the dielectric constant of the host medium, and L is a geometric factor that depends on the shape of the ellipsoidal NP and the direction of E. The dielectric constant of the NP, ϵ, is described by a Drude-Sommerfeld's like model

$$\epsilon = \epsilon_\infty - \frac{\omega_{\mathrm{P}}^2}{(\omega^2 + i\omega\eta)}, \tag{2}$$

where ϵ_∞ is a material-dependent constant and take into account the contribution of the bound electrons to the polarizability, ω_{p} is the plasmon frequency, and η the electronic damping factor. Assuming for simplicity, a linear array of NPs and a near-field approximation for $\mathbf{E}_{i,j}$ yields

$$\mathbf{E}_{i,j} = -\frac{\gamma^{T,L} \mathbf{P}_j}{4\pi \epsilon_0 \epsilon_m d^3}, \tag{3}$$

where d is the distance between NPs, and γ is a constant that depends on the orientation of the NP's array relative to the direction of E, $\gamma^T = 1$ if it is perpendicular and $\gamma^L = -2$ if it is parallel. If we take take into account these considerations, then all $\mathbf{P}$s and $\mathbf{E}^{(\text{ext})}$s can be arranged as vectors $\mathbf{P}$ and $\mathbf{E}$ resulting in the following [28, 29]:

$$\mathbf{P} = \left(\mathbb{I}\omega^2 - \mathbb{M}\right)^{-1} \mathbb{R}\mathbf{E} = \chi \mathbf{E}, \tag{4}$$

where χ is the response function, $\mathbb{M}$ is the dynamical matrix, and $\mathbb{R}$ is a diagonal matrix that rescales the external applied field according to local properties as follows:

$$R_{i,i} = -\epsilon_0 V_i \omega_{\mathrm{p}i}^2 f, \tag{5}$$

with

$$f = \frac{\left[1 - (\epsilon_\infty - \epsilon_{m,i})\left(\omega^2 + i\omega\eta_i\right)/\omega_{\mathrm{p}i}^2\right]}{\left[\epsilon_{m,i} + L_i(\epsilon_\infty - \epsilon_{m,i})\right]}. \tag{6}$$

To understand the physical meaning of f, first note that Eq. 4 resembles that of a set of coupled harmonic oscillators. In the quasi-electrostatic limit, Eq. 3, and for a negligible radiation damping term, see Eq. 9, this similarity is strict for f equal to 1. Thus, this factor essentially accounts

for deviations of the ideal model of coupled harmonic oscillators.

The coupling constants, $M_{i,j} = -\omega_{\chi i,j}^2$ (for $i \neq j$), and the LSP complex square frequencies, $M_{i,i} = \omega_{\text{sp}i}^2 - i\Gamma_i(\omega)$, are given as follows [28, 29]:

$$\omega_{\chi i,j}^2 = \frac{\gamma^{T,L} V_i \omega_{\text{p}i}^2}{4\pi\epsilon_m d_{i,j}^3} f, \tag{7}$$

$$\omega_{\text{sp}i}^2 = \frac{\omega_{\text{p}i}^2 L_i}{\left[\epsilon_{m,i} + L_i(\epsilon_\infty - \epsilon_{m,i})\right]}, \tag{8}$$

and

$$\Gamma(\omega) = \eta\omega + \eta_R\omega^3. \tag{9}$$

where η is the electronic damping and η_R the radiation damping. The electronic damping η can be calculated from the Fermi velocity v_f, the bulk mean free path l_{bulk}, the volume V, and the surface S of the NP by using the Matthiessen's rule $\eta = v_f(1/l_{bulk} - C/l_{eff})$ with $C \approx 1$, and the Coronado-Schatz formula $l_{eff} = 4V/S$ [37]. The value of η_R can be calculated from the ellipsoid's radius a, b, and c, $\eta_R = 2/9(abc/v^3)\omega_P^2 f$, where v is the speed of light in the host medium. This extra damping term appears when the polarizability α is corrected by using the modified long-wavelength approximation, $\alpha' = \alpha[1 - i(2/12\pi\epsilon_0)k^3\alpha]^{-1}$ [36]. In the examples analyzed here, dynamic depolarization is negligible and thus not included in the equations for simplicity.

Retardation effects change the coupling terms which now should be determined by the true dipole-induced electric field, i.e.,

$$\mathbf{E} = \frac{e^{ikd}|P|}{4\pi\epsilon_0\epsilon_m d^3} \left\{ (kd)^2(\hat{d} \times \hat{p}) \times \hat{d} \right. \tag{10}$$

$$\left. + \left[3\hat{d}(\hat{d} \cdot \hat{p}) - \hat{p} \right](1 - ikd) \right\}, \tag{11}$$

where k is the wavenumber in the dielectric, $k = \omega/v$ (where v is the speed of light in the medium), $\hat{d}$ is the unit vector in the direction of $\mathbf{d}$ (where $\mathbf{d}$ is the position of the observation point with respect to the position of the dipole), $\hat{p}$ is the unit vector in the direction of $\mathbf{P}$, and $|P|$ is its modulus. If the system consists of a linear array of NPs where the spheroids axes are aligned with respect to the direction of the array, transversal (T) and longitudinal (L) excitations do not mix, which allows us to preserve the form of Eq. 7 by simply replacing $\gamma^{T,L}$ by $\widetilde{\gamma}^{T,L}$, where

$$\widetilde{\gamma}_{i,j}^L = -2[1 - ikd_{i,j}]e^{ikd_{i,j}}$$
$$\widetilde{\gamma}_{i,j}^T = [1 - ikd_{i,j} - (kd_{i,j})^2]e^{ikd_{i,j}}. \tag{12}$$

We use this final form of the equations in all the calculations shown here. However, the qualitative results do not change by using the quasistatic approximation.

The temporal evolution of the dipolar moments of individual NPs can be evaluated by Fourier transforming the response function $\chi(\omega)$ into $\chi(t)$ and using the convolution theorem as follows:

$$P_i(t) = \sum_j \int_0^t \chi_{i,j}(t - \tau)E_j^{(ext)}(\tau)d\tau. \tag{13}$$

The functions $\chi(t)_{i,j}$ were numerically computed from $\chi(\omega)_{i,j}$ by using a fast Fourier transform algorithm [38]. Here, one must be careful, in case of using active media, of not overpassing the loss-compensation condition as one is always assuming that the response function $\chi_{i,j}$ is square integrable.

Results

Non-Hermiticity of $\mathbb{M}$ and Asymptotic States

In the type of system studied here, frequency and phase locking may appear as a natural consequence of the properties of non-Hermitian matrices. While isolated systems are described by a typical Hermitian dynamical matrix $\mathbb{M}$, where the final state depends on the initial conditions, the presence of an "environment" leads to a non-Hermitian dynamical matrix [28, 29, 39, 41]. This interaction may cause asymptotic states that are independent of the initial conditions. An illustrative example of that is the case of a pair of piano strings in a unison group [42]. There, the slightly detuned strings are coupled through the bridge, which, in turn, is coupled to a dissipative soundboard. Within a certain critical parametric range, this dissipative coupling induces the synchronous oscillation of both strings [42] and gives the piano its characteristic and persistent aftersound. This dissipative coupling can be modeled by an imaginary coupling which, at a critical strength, produces the collapse of the pair of originally mistuned eigenfrequencies into a single tone. Simultaneously, the originally identical dampings split into short- and long-lived modes. The effect of this is that the long time evolution is dominated, for almost any initial condition, by the normal mode whose eigenvalue has the smallest imaginary part.

The same analysis can be straightforwardly applied to plasmonics systems represented by Eq. 4, where the analogy also includes the concepts of dissipative couplings, frequency collapses, and damping's splittings, see Appendix. However, in plasmonic's systems, it is not always obvious which is the asymptotic state of a given system, which makes its control even less obvious. The situation worsens if we consider that usually parameters such as NP's shape and separations are not accurately determined. Besides, unlike the discussed case of coupled piano strings, the amplitude of the oscillations of the LSPs decays so fast that it would

be quite difficult to observe the phase and frequency locking. Therefore, two main features are desirable. The control at will of the asymptotic state of the system and to be able to keep the amplitude of the LSP's oscillations over a long period of time. In the following sections, we will address sequentially each one of these points.

Phase and Frequency Locking

As we mentioned, the plasmonic dynamical matrix $\mathbb{M}$ resembles that of coupled harmonic oscillators. This can be used to analyze certain systems in simple terms as we will see. Assuming the quasi-electrostatic limit, negligible damping terms, and $f \approx 1$, it is easy to evaluate the normal modes of $\mathbb{M}$. In the case of three equal NPs, aligned linearly, and equally spaced, the normal modes can be written as follows: $(P_1 - P_3)/\sqrt{2}$, $(P_1 + \sqrt{2}P_2 + P_3)/2$ and $(P_1 - \sqrt{2}P_2 + P_3)/2$. Where $P1$, $P2$, and $P3$ stand for the dipolar moments in some given direction of NPs 1, 2, and 3, respectively. If the difference in frequency between the NPs of the ends and the central one is small, this expressions are still approximately valid.

Let us analyze this simple example of three aligned NPs and let us assume that we want to ensure an asymptotic state in which the NPs of the ends remain oscillating in anti-phase. In this case, one only need to add a larger damping factor to the middle NP. The normal mode of $\mathbb{M}$ that has zero weight over the NP with a high damping factor, $\approx (P_1 - P_3)/\sqrt{2}$, has a small decay rate compared with the other two, $\approx (P_1 + \sqrt{2}P_2 + P_3)/2$ and $\approx (P_1 - \sqrt{2}P_2 + P_3)/2$, which both have finite weights over the highly dispersive nanostructure (NP 2 in this example). The strategy is then clear, the key to control the phase and frequency locking is the careful designing of the damping factors of NPs in such a way that it leaves one normal mode (the one that will define the desirable phase relationship and frequency) with the smallest, ideally zero, weight over the regions of the array with the largest damping factors.

There are of course several ways of increasing the damping factor of NPs, not only by changing their shape or material but also by "connecting" them to waveguides for example [28, 29]. Here, we use the shape of NPs to control the damping factors. According to the parameters chosen, the radiation damping term is the dominant one for the NP with the high damping factor, while the electronic damping term is the dominant one for the others.

In Fig. 1, we evaluate the temporal evolution of the dipolar moment $P_i(t)$ of each NP by using Eq. 13 in two examples that illustrate how tuning the damping factor of NPs can be used to control the asymptotic state of the system. In these examples, we explicitly take into account the material and shape of NPs, always within the couple
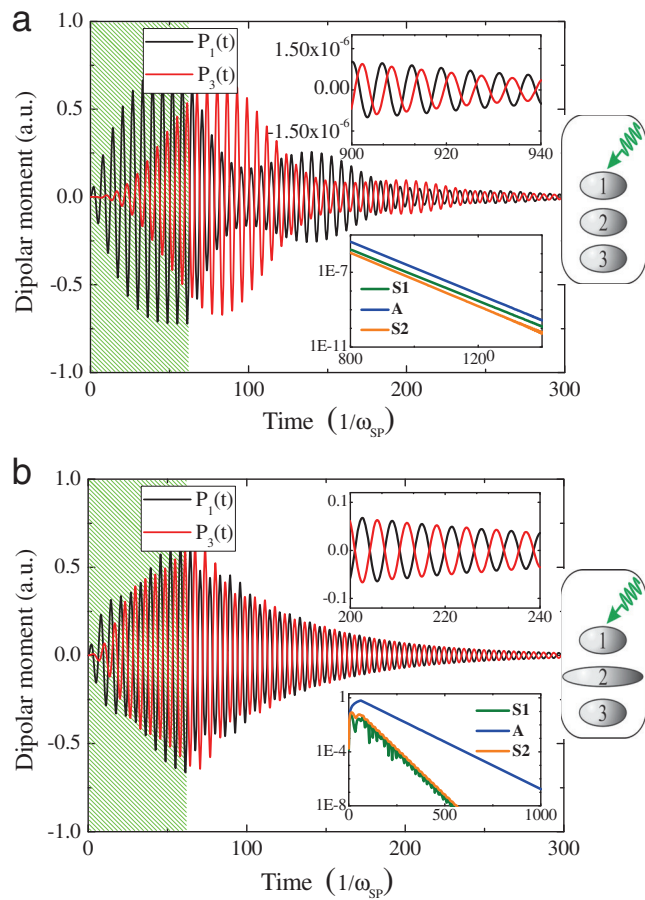

Fig. 1 **a** Dipolar moment P_i of NPs 1 and 3 (in arbitrary units) versus time (in units of ω_{SP}^{-1}) for three aligned and identical NPs. Between $t = 0$ and 62 (mark in *green*), an external field of frequency $\omega = \omega_{SP}$ and direction parallel to the array is applied locally to the first NP to initialize the system. The parameters used correspond to spheroidal Ag's NPs of radii 30, 30, and 8 nm, separated 32 nm, and $\epsilon_m = 1.77$. **b** The same but with the middle NP having a different shape ($90 \times 90 \times 8\ nm$). *Upper insets*: detail of the main figure. *Bottom insets*: detail of the decay rate of different oscillation modes. $S1 = (P_1 + \sqrt{2}P_2 + P_3)/2$, $A = (P_1 - P_3)/\sqrt{2}$, and $S2 = (P_1 - \sqrt{2}P_2 + P_3)/2$. *Side figures*: schemes of the NP's arrays (Color online)

dipole approximation described in "Coupled Dipole Approximation for Ellipsoids with Radiation Damping" and including the full dependence of ω_x^2 and Γ on ω. The results essentially show the above discussed. After the external source is switched off, the LSPs decay very fast, but as indicated in the lower insets, different modes decay at different rates which leads to a natural phase and frequency locking of the LSPs of individual NPs. The asymptotic state of case *a* is not easily seen in the upper inset, but a more careful analysis, depicted in the lower inset, reveals that the mode with the lowest decay rate is "S1." A comparison of Fig. a, b shows that the asymptotic state changes as consequence of the increased damping factor of the middle NP. It should be mentioned that the only role of the external source of electric field is just to initialize the system. This could have been

done in many different ways in the simulation, for example by using a pulse of electromagnetic radiation. However, as long as all normal modes are excited, the final state will be the same, up to a factor in the amplitude of course.

Role of Active Media

As previously mentioned, there is a problem with the phase and frequency locking mechanism described above. Everything occurs too fast. Note that in Fig. 1, the time scale is in units of ω_{SP} of NPs 1 which for the NPs used corresponds to around 0.2 fs. This implies that all the process starts and finishes in less than 0.1 ps approximately. There is a need, then, of keeping the system oscillating for longer periods of time, in order to reasonably envision possible applications. This can be done by embedding the system in an optically active medium.

If the gain of the active medium is below the loss compensation threshold, its effect can be modeled phenomenologically on the basis of classical electrodynamics without taking into account explicitly the quantum dynamics of the chromophores. This is done by considering the medium as a dielectric with a negative imaginary part in the refraction index n. $n = n_0 - i\kappa$ [6–13, 15]. Within this model, the active medium is consistent with a homogeneous distribution of the dye molecules, or nanocrystals quantum dots, and with a wide band approximation for its response.

The wide band approximation implies that the eigenfrequencies of the modes are close compared with the frequency dependence of the active medium. If this condition is not fulfilled, each mode will have a different value of κ or even a null one if the frequency of the mode is far enough from the maximum of the medium's stimulated-emission-spectrum. In this case, the analysis of mode's compensation is direct as it can be based only on mode's frequencies. On the contrary, if the eigenfrequencies of the modes are close enough, such as all modes experience approximately the same value of κ, it is in principle not obvious which mode will be compensated first, and less obvious how to control this. This is why, the wide band approximation allows us to explore alternatives for controlling the system's asymptotic states, beyond the mechanisms based on the frequency response of the active medium or the use of some spatial inhomogeneities in its distribution around the system [24, 25].

As mentioned, it could result not obvious how an active medium would affect the phenomenon depicted in Fig. 1, mainly because n enters not-linearly in the equations, see Eqs. 4–9, and this could in principle changes the expected asymptotic state. However, as we are precisely considering gain media without explicit spacial distribution or frequency dependence, it is reasonable to expect that all modes will be excited similarly. Thus, if there are appreciable differences

in the natural decay rates, the asymptotic states with active medium should be determined directly by them.

Figure 2 shows essentially that. Incorporation of optical gain media does not change the asymptotic states discussed in the previous section, even thought it has been used a value of κ that almost completely compensate losses. In the two examples analyzed, the slowest decaying mode keeps as such, modes "S1" and "A" for cases a and b, respectively. The only effect of the active medium in those examples, besides keeping the system oscillating for longer periods of times, is that it systematically increases even further the differences in the decaying rates, making phase and frequency locking to occur even earlier. As the system remains oscillating for longer periods, it is easier to see in the figures (upper insets) the phase locking and how it is affected by changing the damping factors. In case a, the NPs of the edges (NPs 1 and 3 in Fig. 2) end oscillating in phase, while, if we increase the damping factor of the middle NP as in case c, the NPs of the edges end oscillating in anti-phase. As mentioned before, the reason of that is simply that the anti-phase
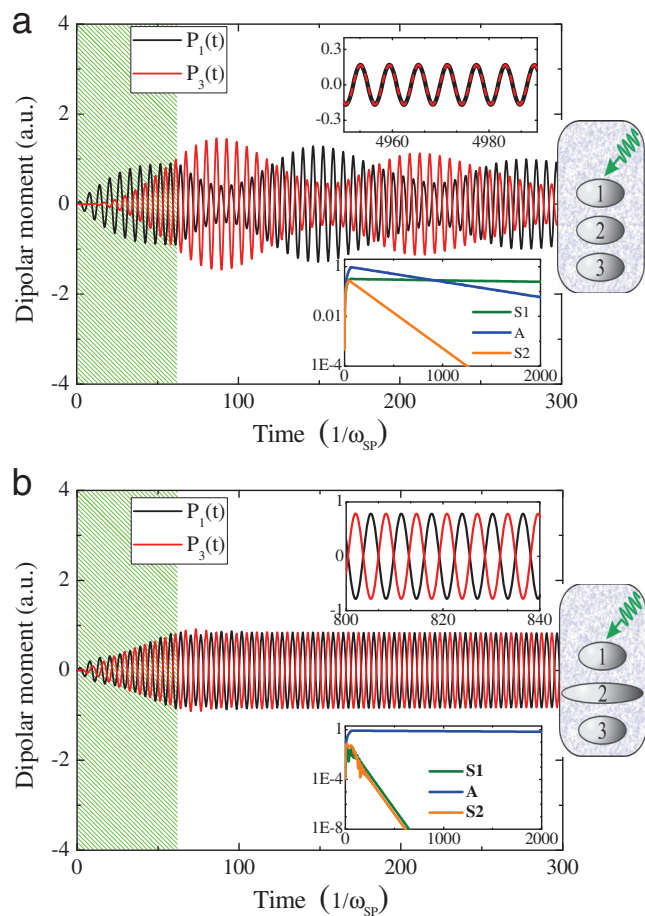

Fig. 2 The same as Fig. 1 but considering an optically active medium with $\kappa = 0.11$ and 0.12 for **a** and **b**, respectively (Color online)

oscillation of the NPs of the edges interfere destructively over the NP of the middle where the largest damping factor is present. The other two normal modes having some weight on the middle NP will increase their decay rate.

Besides the examples shown in the figures, we also tried other possibilities as other NP's arrays or changing the system's parameters. However, the results were always the same, when there are appreciable differences in the decay rates with $\kappa = 0$, which is for example the case of Fig. 1b, a homogeneous active medium is not able to change the expected asymptotic state. Only, for systems like case a of Fig. 1, where the decay rates for $\kappa = 0$ are very close, we observed, for some system's parameters, that the active media changes the expected asymptotic state.

Gain-Loss Compensation

At this point, it is important to discuss about the limiting value of κ, κ_{lim}, for which losses are exactly compensated, and the experimental feasibility of this. The value of κ_{lim} can be evaluated from the poles of Eq. 4 by looking for the pole with the smallest imaginary part. Thus, κ_{lim} is the value of κ for which the imaginary part of this pole equals zero. In some cases, it can be easy to obtain approximate analytical expressions, but in general, one must resort to numerical evaluations.

In case b of Figs. 1 and 2, the eigenvalue of the "A" eigenmode $\omega^2_{\text{eig}-A}$, $(P_1 - P_3)/\sqrt{2}$, can be obtained easily by assuming a wide band approximation as follows:

$$\omega^2_{\text{eig}-A} \approx \omega^2_{\text{SP}} - i\Gamma, \tag{14}$$

where ω^2_{SP} is the LSP resonant frequency of one of the NPs of the ends, and Γ is its damping factor. Then, the value of κ_{lim} can be obtained by using Eq. 8 with $\epsilon_m = n^2$ and assuming a small κ. The result is as follows:

$$\kappa_{\text{lim}} \approx \frac{\Gamma \left[n_0^2 + L \left(\epsilon_\infty - n_0^2 \right) \right]}{2 n_0 \omega^2_{\text{SP}} (1 - L)} \tag{15}$$

which according to the parameters used, $n_0 = 1.33$, $L = 0.689$, $\epsilon_\infty = 3.7$, and $\Gamma/\omega^2_{\text{SP}} \approx 0.032$, gives $\kappa_{\text{lim}} \approx 0.121$.

For case a of Figs. 1 and 2, it is more difficult to obtain simple analytical solutions as ω^2_X also enters into the equations and depends on κ. However, they can always be evaluated numerically. From the simulation, we estimated the value of κ_{lim} as 0.11 and 0.12 approximately for cases a and b, respectively, which should be close to experimental possibilities [18–23, 44–47]. Note the agreement between the numerical and analytical results for case b.

The value of κ is a phenomenological coefficient that represent the property of some media of coherently amplify an electromagnetic field. It is related with the amplification

coefficient g by $g = 4\pi\kappa/\lambda$. Gain media in plasmonics are made of chromophores that overlap spatially and spectrally with the surface plasmon modes of the nanostructure. These chromophores can be semiconductors nanocrystals, dye molecules, rare-earth ions, or electron-hole excitations of a bulk semiconductor. The gain coefficient can be written as $g = N\sigma_e$, where N is the concentration of electron-hole pairs in the case of semiconductors or the concentration of molecules and their population inversion in the case of dye molecules. The symbol σ_e is the stimulated emission cross section which, in turn, depends on the dipolar moment of the transition [6–17].

Here, we should clarify one point. Up to now, we have been discussing and comparing the decay rates of different modes that have always the same direction of the electric field, parallel to the array. However, there are two other set of modes, those with the electric field perpendicular to the array that can also enter in the analysis of the system's asymptotic state. If the dipolar moment of the transition of the molecules or semiconductors nanocrystals that constitute the active media have a preferential direction, then the media can only feedback some modes, those with a finite overlap between the mode's electric field and the dipolar moment [15–17]. In this case, only some modes, ideally those that oscillate in the preferable direction, should be considered. On the contrary, if the dipolar moment of the transition has a random orientation, then one has to analyze the full picture, i.e., the whole nine modes for the arrays. In this last case, the shape of the NPs acquires a central role because it determines in which direction the system will remain oscillating. To see that, note that the L_i factor of Eq. 1 depends on both the shape of the NP and the direction of electric field, and this parameter enters, not only in eigenfrequency of the mode, but also in the damping term Γ through η_R and f.

For example, let us consider a system of three equal NPs of 30 x 20 x 8 nm aligned in the direction of the minor axis and separated 24 nm. Here, the mode that is compensated in the first place by the active medium is that where all LSPs are oscillating synchronous in phase and parallel to the major axis. In this case, $\kappa_{\text{lim}} \approx 0.024$. The equivalent modes but for the other directions, those where the LSPs oscillate in phase and parallel to the second largest axis and to the minor axis, have a value of κ_{lim} of approximately 0.029 and 0.073, respectively.

Amplitude Locking

According to our equations up to now, for $\kappa > \kappa_{\text{lim}}$, $P(t)$ should grow exponentially at infinitum, which is of course not realistic. At some point, the pumping mechanism that keeps the inversion population must be overcome by the decay rate of the molecules in the excited state decaying

toward their fundamental state. The realistic situation is that the amplitude of the surface plasmon oscillations should stabilize at some point. This is so because the stimulated emission that depletes the excited states depends on $|E|^2$ which, in turn, depends on P_i, while the mechanism that restore the inversion population is fixed and independent of P_i [15–17].

A complete treatment would require to solve the quantum mechanics dynamics of each chromophore under the influence of the electromagnetic field corresponding to its position and the coupled equation of motion of the surface plasmon dynamics. This is beyond the scope of this work and besides was already addressed by other authors in the context of spasers [15, 17]. The important result of these previous works, for the present purposes, is that the system evolves in a somehow complex way, until a stationary regime is reached. This stationary regime corresponds to a net amplification equals zero, which means that gain exactly compensate losses [14–17], a condition expressed in our case by Eq. 15 in terms of κ_{lim}. Essentially, the convergence towards a stationary regime where losses are compensated, implies amplitude locking. The asymptotic value of the amplitude could be complex to evaluate but the important point is that, sooner or latter, it is reached and it is nonzero for $\kappa_{initial} > \kappa_{lim}$ and initial conditions different from the trivial one, $P_i = 0$. The other important point is that, once the system is in the stationary state regime, the inversion population freezes, fixating the gain coefficient g and thus κ, at $\kappa = \kappa_{lim}$. Then, independently of how or when this stationary regime is reached, in the end one should see the type of behaviors showed in the context of Fig. 2, i.e., different normal modes are compensated differently by the active medium. Therefore, while the slowest decaying mode is exactly compensated, the others will be undercompensated which will inevitably lead to a phase, frequency, and also amplitude locking. Note that, because of this, the plasmonics systems studied can be considered as a new example of synchronization.

The above analysis has also another important consequence, gain medium cannot, in general, exactly compensate the losses of all eigenmodes at the same time. Let us assume the system has three eigenmodes each one with different values of κ_{lim}; $\kappa_1 < \kappa_2 < \kappa_3$. Then, if one try to compensate the second or the third modes , $\kappa = \kappa_2$ or $\kappa = \kappa_3$, the first one will be overcompensated which can not define a stationary state as it should grow indefinitely. The realistic situation is that the inversion population of the active medium will be depleted by the increasing electromagnetic field of the first mode, reducing the value of κ until it reaches κ_1. As this argument is very general, we believe its consequences should be present in the majority of this kind of systems provided that the necessary ingredients are present. The eigenfrequencies of the modes must

be close enough compared with the frequency response of the medium and different modes should share somehow the same dye molecules or semiconductor nanocrystals. We plan to address this interesting issue in a future work.

Figure 3a, b show the electric field generated by the examples shown in Figs. 1 and 2 for $t \to \infty$. The former corresponds to the system with three equal NPs and the latter to the system with the middle NP having a larger damping factor. Note the great differences in the emitted electric fields. The upper case shows the typical interference patterns of a punctual dipolar source, while the lower one shows that of a quadrupole. This example highlight the fact that amplitude locking becomes our system into, not only another example of synchronization, but also a nanometric source of both evanescent and propagating waves with a predetermined and controllable interference pattern.

Generalization to More Complex Structures

The proposed synchronization mechanism can be easily extended to more complex nanostructures. The key is to build the system such as all normal modes but one have some weight on the highly dispersive NPs, the middle one in Fig. 2b for example. Then, if the damping factor of the highly dispersive NP is large enough, the slowest decaying
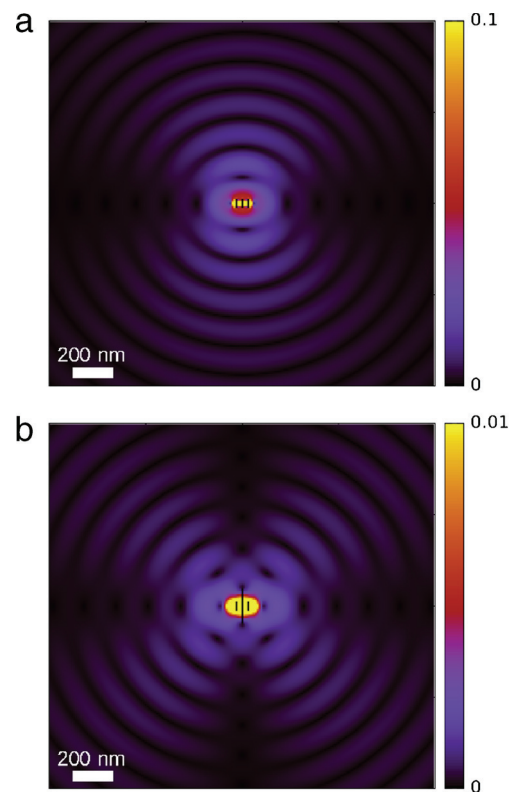

Fig. 3 $|E|^2$ for the asymptotic state of case (**a**) and (**b**) of Fig. 2. The strength of $|E|^2$ is normalized to its maximum value in each figure
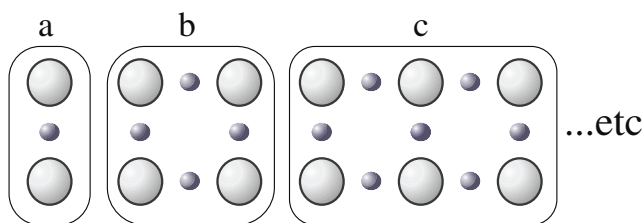
Fig. 4 Schemes of others NP's arrays. *Small* spheres stand for NPs with large damping factors while the *large* ones represent NPs with small damping factors (Color online)

normal mode, which will control the relative phases of the LSP in the asymptotic state, will be that having the smallest weight over these NPs. In Fig. 4, we present just one possible set of examples of that for NP's arrays of arbitrary size. The examples assume nearest neighbors interactions. The small spheres represent equal NPs with large damping factors while the large ones represent equal NPs with small damping factors. In all these cases, one can show that there is always one eigenvalue of $\mathbb{M}$ that has zero weight over the small NPs. This normal mode corresponds to that where the LSP of the large NPs oscillates in anti-phase with respect to their nearest large-NPs neighbors. Thus, as this mode will have the slowest decay rate, it will determine the phase locking at long time. Others asymptotic states are also possible in those systems. One only has to evaluate the weight of individual NPs on each normal mode and, based on that, increases selectively the damping factors of certain NPs to achieve the desired asymptotic state.

Conclusions

In this work, we have shown a simple way of controlling phase and frequency locking of the self-sustained oscillation of NP's LSPs by tuning the damping factors of individual NPs. Furthermore, we have shown that it should be possible to keep the system oscillating with constant amplitude by including optically active media properly tuned. We interpret this as a new example of synchronization as we are in the presence of self-sustained oscillating objects, clearly separable, that depict phase, frequency, as well as amplitude locking, consequence of their mutual interaction. Since it is possible to control the asymptotic state of these NP arrays with self-sustained LSP, our approach is a general way of designing the interference patterns of sources of optical fields in the subwavelength scale. This can surely find applications in optoelectronic, nanoscale lithography, and probing microscopy. In addition, the proposed method can naturally be combined with other alternatives, such as using the frequency dependence of the active medium or controlling its spatial distribution.

Appendix: Dissipative Couplings and Dynamical Phase Transitions

We mentioned that in the case of coupled piano strings, there is a dissipative coupling between the strings which can be modeled by an imaginary coupling term in the dynamical matrix $\mathbb{M}$. Pure imaginary, or at least complex, couplings have interesting effects on the properties of the eigenvalues of $\mathbb{M}$. At some critical values of the system's parameters, there can be a collapse of the real part of the eigenvalues of $\mathbb{M}$ and a bifurcation of their imaginary part at points called "exceptional points." There, among other effects, $\mathbb{M}$ becomes singular and the system's eigenvectors behave oddly in their surroundings [39, 40]. Since the dynamical observables have a nonanalytic dependence on the system's parameters, this results in what is called a dynamical phase transition, DPT [28, 29, 39, 41].

In the case of plasmonics systems, as those showed in this work, the complex coupling can be seen as just the consequence of the effective interaction between two parts of a system connected through a bridging dissipative subsystem. For example, if we have three NPs aligned, one can always calculate an effective coupling between the NPs at the ends [43]. The result of this is a complex effective coupling, consequence of the damping term of the NP in the middle [28, 29].

Figure 5 shows that the eigenvalues of $\mathbb{M}$ present a collapse of their real part accompanied by a splitting of their imaginary part. Just as in the example of the coupled piano strings. This case corresponds to a very large value of the damping term of the middle NP and a mistuning parameter, δ, below a critical value. Here, it should be mentioned that what really sets the decay rates are the imaginary part of the poles, $\mathrm{Im}\left(\omega_{\mathrm{pole}}\right)$, of the response function $\chi(\omega)$, and not the imaginary part of the eigenvalues of $\mathbb{M}$. In the wide band approximation, these last coincides with $\mathrm{Im}\left(\omega_{\mathrm{pole}}^2\right)$. This distinction can be quite irrelevant in some situations but becomes fundamental in others. In Fig. 6, we consider the case of two interacting NPs. We can see that although the eigenvalues of $\mathbb{M}$ have exactly the same imaginary part, which would preclude the synchronization mechanism depicted in the main section of the article, there is a difference in the imaginary part of ω_{pole}. Although this difference is very small, as compared with the case shown in Fig. 5, it is enough to give rise to a characteristic asymptotic state and,

Fig. 5 Panels **a**, **b** are, respectively, the real and imaginary part of ω_{pole}^2, the eigenvalues of $\mathbb{M}$; while panels **b**, **d** are, respectively, the real and imaginary part of ω_{pole}, the poles of χ. The system consists of three aligned NPs with $\delta = \omega_{SP1}^2 - \omega_{SP3}^3$, where 1 and 3 stand for the NPs of the edges. Only nearest neighbor couplings are considered, $\omega_X^2 = 0.2$, $\omega_{SP}^2 = 1$ (for $\delta = 0$), and $\Gamma = 0.03$ for all NPs except for the middle one where $\Gamma = 0.7$ (Color online)
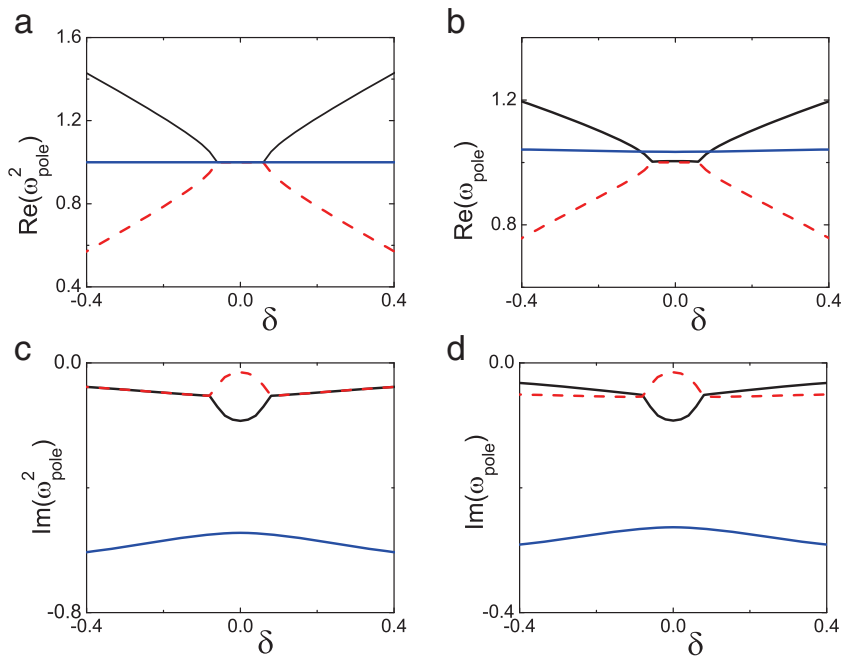
thus, it can be used to induce a phase and frequency locking. In this example, the mode with the longest lifetime will be the antisymmetric one. This, at sufficiently long times, implies that the LSPs of both NPs will end oscillating in anti-phase.

In general, systems with dynamical phase transitions are expected to have large differences in the imaginary parts of the eigenfrequencies, as in the case of coupled piano strings or in the example shown in Fig. 5. However, phase and frequency locking is not an exclusive phenomenon of this situation. For the particular case of metallic nanoparticle arrays, the value of the damping terms needed to achieve the DPT described here are far from the realistic situation, at least for metallic NPs. Thus, the cases discussed in the main section of the article correspond to systems that do not present a DPT.

Fig. 6 The same as Fig. 5 but for a system of two NPs with equal damping, $\Gamma = 0.03$. Notice that in spite of the small differences in decay rates as compared to those in Fig. 5, they can be enough to produce an observable phase locking through the use of an active medium (Color online)
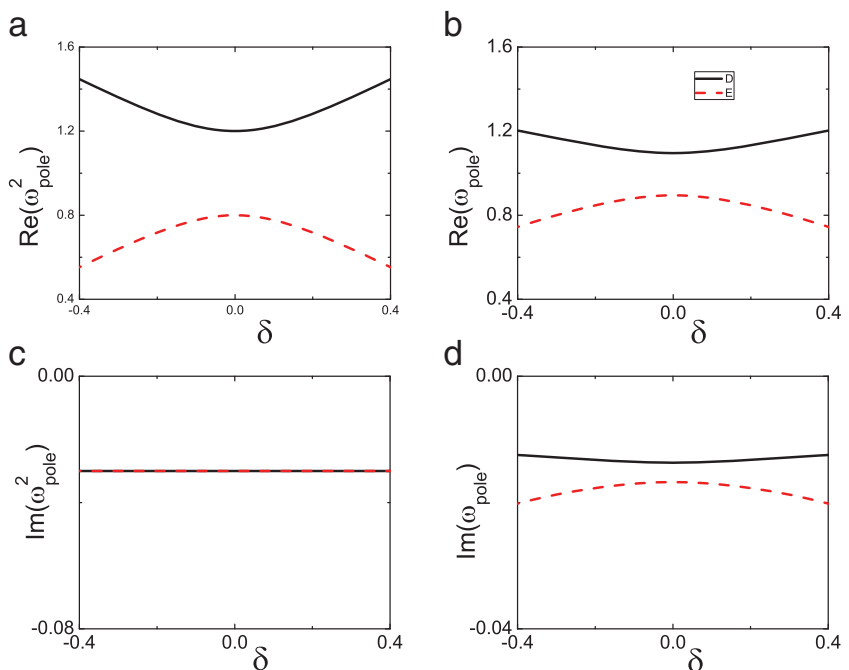
References

1. Maier SA (2007) Plasmonics: fundamentals and applications. Springer, New York
2. Novotny L, Hecht B (2007) Principles of nano-optics. Cambridge Press, Cambridge
3. Coronado E, Encina E, Stefani FD (2011) Optical properties of metallic nanoparticles: manipulating light, heat and forces at the nanoscale. Nanoscale 3:4042
4. Halas N, Lal S, Chang W-S, Link S, Nordlander P (2011) Plasmons in strongly coupled metallic nanostructures. Chem Rev 111:3913
5. Ebbesen T, Genet C, Bozhevolnyi S (2008) Surface-plasmon circuitry. Phys Today 61:44
6. Cao Y, Wei Z, Li W, Fang A, Li H, Jiang X, Chen H, Chan CT (2013) Light amplification with low-gain material: harvesting harmonic resonance modes of surface plasmon polaritons on a magnetic meta-surface. Plasmonics 8:793
7. Hess O, Pendry JB, Maier SA, Oulton RF, Hamm JM, Tsakmakidis KL (2012) Active nanoplasmonic metamaterials. Nat Mater 11:573
8. Tao J, Wang QJ, Huang XG (2011) All-optical plasmonic switches based on coupled nano-disk cavity structures containing nonlinear material. Plasmonics 6:753
9. Krasavin A, Phong Vo T, Dickson W, Bolger P, Zayats A (2011) All-plasmonic modulation via stimulated emission of copropagating surface plasmon polaritons on a substrate with gain. Nano Lett 11:2231
10. Kottos T (2010) Optical physics: broken symmetry makes light work. Nat Phys 6:166
11. Wuestner S, Pusch A, Tsakmakidis KL, Hamm JM, Hess O (2010) Overcoming losses with gain in a negative refractive index metamaterial. Phys Rev Lett 127401:105
12. Noginov M, Zhu G, Belgrave A, Bakker R, Shalaev V, Narimanov E, Stout S, Herz E, Suteewong T, Wiesner U (2009) Demonstration of a spaser-based nanolaser. Nature 460:1110
13. Li Z-Y, Xia Y (2010) Metal nanoparticles with gain toward single-molecule detection by surface-enhanced Raman scattering. Nano Lett 10:243
14. Bergman DJ, Stockman MI (2003) Surface plasmon amplification by stimulated emission of radiation: quantum generation of coherent surface plasmons in nanosystems. Phys Rev Lett 90:027402
15. Stockman MI (2010) Spaser as nanoscale quantum generator and ultrafast amplifier. J Opt 12:024004
16. Stockman MI (2011) Spaser action, loss compensation, and stability in plasmonic systems with gain. Phys Rev Lett 106:156802
17. Fang A, Koschny T, Soukoulis CM (2010) Lasing in metamaterial nanostructures. J Opt 12:024013
18. Oulton RF, Sorger VJ, Zentgraf T, Ma R-M, Gladden C, Dai L, Bartal G, Zhang X (2009) Nature 461:629
19. Noginov M, Zhu G, Belgrave A, Bakker R, Shalaev V, Narimanov E, Stout S, Herz E, Suteewong T, Wiesner U (2009) Demonstration of a spaser-based nanolaser. Nature 460:1110
20. Hill MT et al (2009) Lasing in metal-insulator-metal subwavelength plasmonic waveguides. Opt Express 17:11107
21. Yong Suh J, Hoon Kim C, Zhou W, Huntington MD, Co DT, Wasielewski MR, Odom TW (2012) Plasmonic bowtie nanolaser arrays. Nano Lett 12:5769
22. Ma R-M, Yin X, Oulton RF, Sorger VJ, Zhang X (2012) Multiplexed and electrically modulated plasmon laser circuit. Nano Lett 12:5396
23. Wu C-Y, Kuo C-T, Wang C-Y, He C-L, Lin M-H, Ahn H, Gwo S (2011) Plasmonic green nanolaser based on a metal-oxide-semiconductor structure. Nano Lett 11:4256
24. Li J, Zhang Y, Mei T, Fiddy M (2010) Surface plasmon laser based on metal cavity array with two different modes. Opt Express 18:23626
25. Kitur JK, Podolskiy VA, Noginov MA (2011) Stimulated emission of surface plasmon polaritons in a microcylinder cavity. Phys Rev Lett 106:183903
26. Pikovsky A, Rosenblum M, Kurths J (2001) Synchronization: a universal concept in nonlinear sciences. Cambridge University Press, Cambridge
27. Hugenii C (1673) Horoloquium oscilatorium. Apud F. Muguet, Parisiis
28. Bustos-Marún RA, Coronado EA, Pastawski HM (2010) Buffering plasmons in nanoparticle waveguides at the virtual-localized transition. Phys Rev B 82:035434
29. Bustos-Marún RA, Coronado EA, Pastawski HM (2012) Excitation-transfer plasmonic nanosensors based on dynamical phase transitions. J Phys Chem C 116:18937
30. Brongersma ML, Hartman JW, Atwater HA (2000) Electromagnetic energy transfer and switching in nanoparticle chain arrays below the diffraction limit. Phys Rev B 62:R16356
31. Citrin DS (2004) Coherent excitation transport in metal-nanoparticle chains. Nano Lett 4:1561
32. Burin L, Cao H, Schatz GC, Ratner MA (2004) High-quality optical modes in low-dimensional arrays of nanoparticles: application to random lasers. J Opt Soc Am B 21:121
33. Garcia de Abajo FJ (2007) Colloquium: light scattering by particle and hole arrays. Rev Mod Phys 79:1267
34. Malyshev AV, Malyshev VA, Knoester J (2008) Frequency-controlled localization of optical signals in graded plasmonic chains. Nano Lett 8:2369
35. Jones RC (1945) A generalization of the dielectric ellipsoid problem. Phys Rev 68:93
36. Kelly K, Coronado EA, Zhao L, Schatz GC (2003) The optical properties of metal nanoparticles: the influence of size, shape, and dielectric environment. J Phys Chem B 107:668
37. Coronado EA, Schatz GC (2003) Surface plasmon broadening for arbitrary shape nanoparticles: a geometrical probability approach. J Chem Phys 119:3926
38. Press W, Teukolsky S, Vetterling W, Flannery B (1998) Numerical recipes in fortran 77: the art of scientific computing. Cambridge University Press, Cambridge
39. Rotter I (2009) A non-Hermitian Hamilton operator and the physics of open quantum systems. J Phys A Math Theor 42:153001
40. Gilary I, Mailybaev AA, Moiseyev N (2013) Time-asymmetric quantum-state-exchange mechanism. Phys Rev A 88:R010102
41. Pastawski HM (2007) Revisiting the Fermi Golden Rule: quantum dynamical phase transition as a paradigm shift. Phys B 398:278
42. Weinreich G (1977) Coupled piano strings. J Acoust Soc Am 62:1474
43. Pastawski HM, Medina E (2001) 'Tight binding' methods in quantum transport through molecules and small devices: from the coherent to the decoherent description. Rev Mex Fis 47s1:1
44. Pisignano D, Anni M, Gigli G, Cingolani R, Zavelani-Rossi M, Lanzani G, Barbarella G, Favaretto L (2002) Amplified spontaneous emission and efficient tunable laser emission from a substituted thiophene-based oligomer. Appl Phys Lett 81:3534
45. Carrere H, Marie X, Lombez L, Amand T (2006) Optical gain of InGaAsN/InP quantum wells for laser applications. Appl Phys Lett 89:181115
46. Seidel J, Grafström S, Eng L (2005) Stimulated emission of surface plasmons at the interface between a silver film and an optically pumped dye solution. Phys Rev Lett 94:177401
47. Noginov MA, Zhu G, Mayy M, Ritzo BA, Noginova N, Podolskiy VA (2008) Stimulated emission of surface plasmon polaritons. Phys Rev Lett 101:226806